

In situ measurements of NO, NO₂, NO_y, and O₃ in Dinghushan (112°E, 23°N), China during autumn 2008

Yang Sun^{a,b}, Lili Wang^b, Yuesi Wang^{b,*}, Deqiang Zhang^c, Liu Quan^b, Xin Jinyuan^b

^a Lanzhou University, Lanzhou 730000, China

^b State Key Laboratory of Atmospheric Boundary Layer Physics and Atmospheric Chemistry (LAPC), Institute of Atmospheric Physics, Chinese Academy of Sciences, Beijing 100029, China

^c South China Botanical Garden, Chinese Academy of Sciences, Guangzhou 510650, China

ARTICLE INFO

Article history:

Received 14 September 2009

Received in revised form

10 March 2010

Accepted 11 March 2010

Keywords:

NO

NO₂

NO_x

OPE

SPM

ABSTRACT

Measurements of O₃, NO, NO₂, and NO_y mixing ratios were carried out at a station-Dinghushan in Guangdong province of China from Oct. 18th, 2008 to Nov. 7th, 2008. This research shows that under conditions of a strong subtropical high (temperature high, relative humidity low), on Oct. 29th, 2008 the Dinghushan station observed severe photochemical pollution. The Maximum hour average concentration of O₃ reached 128 ppbv, and the serious photochemical pollution is caused by superposition of local photochemical reaction and regional transport. The observation that NO_x ozone production efficiency (OPE) values for high O₃ pollution on Oct. 29–30th, 2008 were 10.5 and 15, which were more than the values of the city source region and lower than that of the surrounding clean areas. It means the sensitivity of O₃ generated was transitioning from VOCs limited condition to NO_x-limited regime. By applying a Smog Production Model, the results show that the extent of reaction values less than 0.6 were occurred on 17 days during campaign, and 13 days for the extents of reactions more than 0.6. However, there were no data with values over 0.8, which indicates that the observation station represent a VOCs sensitive system during campaign. Analysis of the extents of reactions and wind data show that the pollution is mostly subject to a southeasterly airflow influence.

© 2010 Elsevier Ltd. All rights reserved.

1. Introduction

During the past 20 years, Guangdong province in south China has undergone a rapid increase in economic development. The number of automobiles increased from 1 to 5.4 million between 1995 and 2008. Due to the increasing industrial activities and the number of automobiles, the emission of VOCs (volatile organic compounds) and NO_x = (NO + NO₂) have show significant increase in this region. It is well known that tropospheric ozone originates mostly from the photochemical reactions of volatile organic compounds (VOCs) and oxides of nitrogen (NO_x) [National Research Council, 1991]. NO_x plays the role of catalyst in the chain reactions for ozone production. In addition, NO_x is also one of the major terminators of free radicals. The NO_x emitted from fossil fuel combustion has a lifetime of less than a day against oxidation to HNO₃ and peroxyacetylnitrate (PAN) (Raivonen et al., 2009; Penga et al., 2006; Carl et al., 2001; Thomas et al., 2005; Guangfeng and Jerome, 2004; Cassandra et al., 2006). It be referred to the sum of

NO, NO₂, N₂O₅, HNO₃, PAN, and other minor NO_x oxidation products as total reactive nitrogen (NO_y). NO_y also plays a central role in the aeronomy of the atmosphere, in tropospheric pollution, and in stratospheric ozone loss. Significant effort has been devoted to accurate and comprehensive measurements of NO_y and its component species (Paul et al., 2008; Ariel et al., 2005; Zhang et al., 2008; Moore et al., 2001). We also use NO_z (NO_y–NO_x) to analyze production of ozone for different role in chemistry in paper.

In this study, we investigate the O₃, NO, NO₂, and NO_y measured in the Dinghushan in Pearl River Delta region between October 18th and November 7th. The paper will be organized in the following way. In Section 2, we will describe the instruments and measurements, including the part of photolytic conversion of NO₂. In Section 3, the measured results are analyzed to study the characterizations of ozone and the NO_x, NO_z and NO_y pollutants and chemical processes which control the O₃ formation. Some photochemical indicator ratios were calculated and the extent of reaction in the SPM was estimated. The VOCs- or NO_x sensitive regime to the formation of ozone was identified in this region. In Section 4, we formulate some conclusions and plans for further studies.

* Corresponding author.

E-mail address: wys@mail.iap.ac.cn (Y. Wang).

2. Methods

Dinghushan Forest Ecosystem Research Station, Chinese Academy of Sciences (DFERS), also sometimes referred to as Dinghushan Biosphere Reserve, (112°30′39″–112°33′41″E, 23°09′21″–23°11′30″N) is located in the mid-part of Guangdong Province in south China in a northeastern suburb of Zhaoqing, ~84 km away from Guangzhou (Fig. 1). It occupies 1133 km², covered mostly by hills and valleys. The altitude of the reserve ranges nearly from 100 to 700 m above sea level, with the highest point (1000 m) at Jilongshan (<http://dhs.scib.ac.in>).

Ozone was measured using a commercial UV photometric analyzer (Thermo Environmental Instruments (TEI) Inc.; Model 49i) with a detection limit of 0.5 ppbv and a precision of 1 ppbv. For NO₂ the most widely used method transform other nitrogen-containing compounds such as HNO₃, PAN, etc. Even low temperature catalytic molybdenum converts to a considerable extent. In this research, NO₂ measurements methods using photolytic conversion of NO₂ to NO followed by NO/O₃ chemiluminescence and UV differential optical absorption spectroscopy. The PLC 860 was used which is a photolysis converter Made by ECO PHYSICS, The PLC 860 enables the measurement of NO₂ at much lower concentration levels and is far more selective than would be possible using other converters based on chemical, thermal, or catalytic technology (Mannschreckl et al., 2004). The NO_y analyzer is based on the Thermo Model 42C NO–NO₂–NO_x Trace Level Analyzer. The major difference is utilization of an external molybdenum converter, which minimizes sample transport distances, thereby allowing the NO_y analyzer to measure more compounds that would otherwise not be measured by using an internal converter. An automatic meteorological observation tower called Milos520 (Vaisala, Finland) is located at the same site, and was used to observe atmospheric pressure, temperature, relative humidity, dew point, and the speed and direction of wind in the atmosphere at ground-level.

3. Results and discussion

3.1. Overview of the time series

Fig. 2 shows the time series of O₃, NO, NO₂, and NO_x mixing ratios and meteorologic data for the campaign period. The data

analysis in this study was based on the hourly averaged mixing ratio of each species. To focus our discussion on the formation of high-ozone events, we examine incidents with daily maximum 1-h averaged [O₃] greater than 100 ppbv. This level is roughly equivalent to a China Class II standard (200 μg m⁻³) (Environmental Air Quality Standard GB3095-1996, 2000 revised version).

According to the weather differences. The observation period is divided into three stages.

In first stage, from October 18th to November 1st, the daily variation of relative humidity and temperature were regularity and average value were 70% and 26.2 °C respectively. According to the report of China Meteorological Administration (CMA) (<http://www.cma.gov.cn>), Dinghushan is characterized by a continuously strong subtropical high with reduced influence of air mass passing Nanling Mountains from the north; the Guangdong province is not obviously affected by the cold air. So precipitation is low, temperatures are high, and the air is dry. Under this condition the average daily temperature (26.2 °C) is significantly higher than climatology (24.0 °C) by 2.2°. Only on October 23rd, there was sporadic rain observed, and the concentration of pollutants is significantly reduced due to wash-out by precipitation. In most of time, [O₃] concentration may reach a high level when sky is clear and surface wind speeds are small, which is attributed to the strong solar radiation. This kind of weather has been found to facilitate ozone production (Wang et al., 1998). So the daily maximum magnitude becomes higher. While on October 29th ozone achieves the largest average value of 128 ppbv (the following section will analyze the case in detail), [NO] stays low, and there is weak peak traffic which appears everyday. [NO₂] does not reach high values with the relatively slow changes. On October 29th a sharp sudden increasing was occurred; and NO_x have remarkable peak value of 15.3 ppbv on October 28th.

During the second stage, from November 1st to November 9th, the relative humidity is high (average value was 81%), with relative low temperature and weak solar radiation due to the rainfall events occurred between November 1st to 6th, resulting in a small daily variation of chemical compounds during that period. Continuous overcast and rainy weather is not conducive to the spread of a pollutant, while the O₃ photochemical production rates are low. Therefore, O₃, NO_x, and other photochemical pollutants reach their lowest concentrations, while NO and NO₂

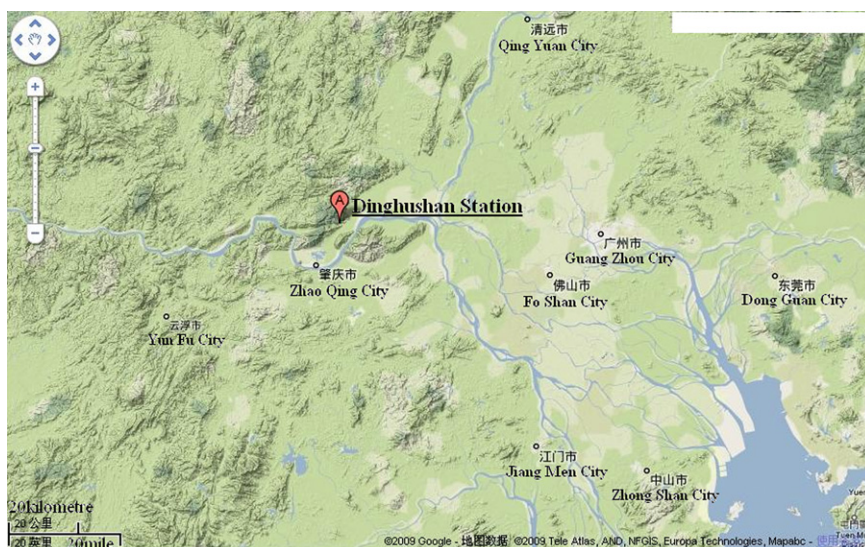


Fig. 1. Sampling location in West of Guangdong province south of China.

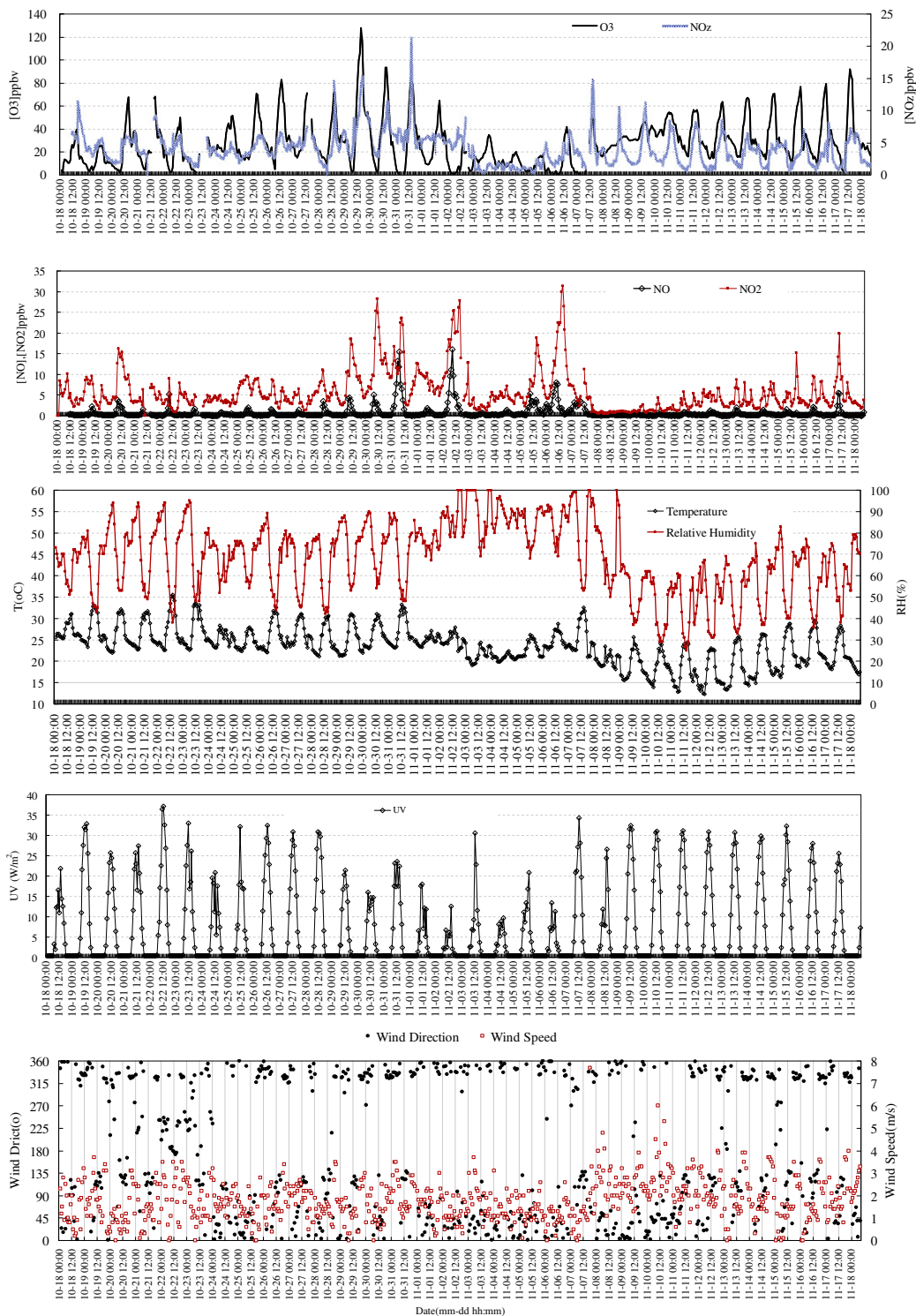


Fig. 2. The time series mixing ratios of O₃, NO, NO₂, and NO_z and meteorological data for the 2008 campaign period.

have relative high concentrations when precipitation is low during this period.

Then in the third stage, from November 9th to 18th, the value of relative humidity and temperature decline obviously and daily variation was significant, because of the strong solar radiation. A strong ground-level cold air event on the afternoon of November 8th passes over the mountains from north to south Nanling and impacts Guangdong province region. This is accompanied by

moderate rain, the region is affected and controlled by a cold ridge of high pressure, and on the 9th there is substantially cold air. From November 11th to 13th the cold high pressure begins to weaken, and cold air mass gradually goes eastward, followed by a three-day long control from a variable ridge. Strong cold air on the night of 17th has impacts on Guangdong province from north to south. Later, the region is controlled by a cold ridge of high pressure. In this period, concentrations of various pollutants are very low,

for [NO] and [NO₂] particularly. [O₃] and [NO₂] were background concentrations of air mass that transport from the north. NO₂ is the basic element of NO_x. O₃ has no significant daily change in the pre-phase, but from November 11th onward there begins a steady growth with strong regularity. And this continues for a week, indicating the stability of the circulation pattern, which is in favor of carrying out the photochemical reactions. But since it is the fall season, with less other conditions conducive to the reactions, there are no days exceeding the environmental standard. Therefore, under the control of cold high pressure, the lower level atmosphere shows no major changes in the weather situation. The temperature is high (20.4 °C) and relative humidity is low (54.3%).

The data of NO, NO₂, NO_x and O₃ have been regrouped into three stages and averaged daily values are plotted in Fig. 3. It can be seen from Fig. 3 that the daily variations of [NO] were similar in all the three stages with one single peak occurring at 0800 Local Standard Time (LST). The second stage has maximal hour concentration of 4 ppbv. The behaviors of [NO₂] in the first and the last stages were similar with one peak in the morning (0900 LST) and another in the afternoon (1800 LST). In the second stage, the bi-peak shape is not clear, with maxima peak of 11 ppbv occurring at 1500 LST. [NO_x] show its maxima at 1400 to 1500 LST. A maximum [NO_x] of 9 ppbv is seen in the first stage. The daily [O₃] reach its maxima at local afternoon (1500 LST) with higher hour value of about 70 ppbv in first and last stages. A relative lower maximum value of 35 ppbv is seen in the second stage.

3.2. Episode (2008-10-29)

On October 29th, 2008, Dinghushan station observed a serious photochemical pollution. The largest hourly mean [O₃] reached 128 ppbv, beyond the China Class II standard about 28% (a mean 1-h value of 200 μg m⁻³ ≈ 100 ppbv, from the Environmental Air Quality Standard GB3095-1996, 2000 revised version). Pollutant and meteorological data are analyzed as follow and plotted Fig. 4.

Before October 29th 0400 LST, there are not much of additional input of NO to decrease [O₃] in rural area in midnight, and ozone that produced in daytime could be accumulated (Ariel et al., 2005), at that time [NO₂] and [NO_x] decline slowly, and [NO₂] was a dominant factor in the decline. This is because of dry deposition at night, after 0400LST, when [NO] and [NO₂] started to increase rapidly, and the sum of [NO₂], [NO] and [NO_x] increased to a maximum (28.2 ppbv) at 1000 LST, [NO₂] play a dominant role in it. At the same time, [NO] started to rise from 0600LST and increased to maximum (4.4 ppbv) at 0800LST, then [NO] maintained under 1 ppbv during the October 29th day.

The change of NO, NO₂ and NO_x in remote area is different from that in urban areas in the morning, a stable boundary layer vertical diffusion is weak, leading to the accumulation of nitrogen oxides emitted in boundary layer. Therefore, the NO and NO₂ concentrations in the city would decrease rapidly because of the increase of the height of boundary layer. Dinghushan belongs to remote mountainous area, where is weak emission source in boundary layer at night, and since the mixed layer was uplifted in the morning, vertical mixture would take smoke plumes from the sky to the ground to make the concentration of pollutants, such as NO₂ and NO_x, increase rapidly. From Fig. 4, the relative humidity was dropped rapidly around Oct.29th 0700 LST shows that uplifted vertical movement in different mixed layer changed property of surface layer air mass. 0700–0900 LST appeared quasi-static wind conditions in 3 h, at the same time, the UV radiation became strong, relative humidity began to decline that showed the exchange of turbulence was enhanced, which are conducive to photochemical reactions, therefore, [O₃] started to increase rapidly, there was a small amount of local traffic emissions NO input atmosphere at 0600 LST, and thus NO₂, O₃, NO_x, began to rise overall later. Because of the stable boundary layer, weak convection reduced the importation of precursor to produce a small peak that NO₂ changed to NO_x at 0800 LST. Then the disturbance of weak surface wind (0.5–1 m s⁻¹) from the NNE was helpful to import the precursors to

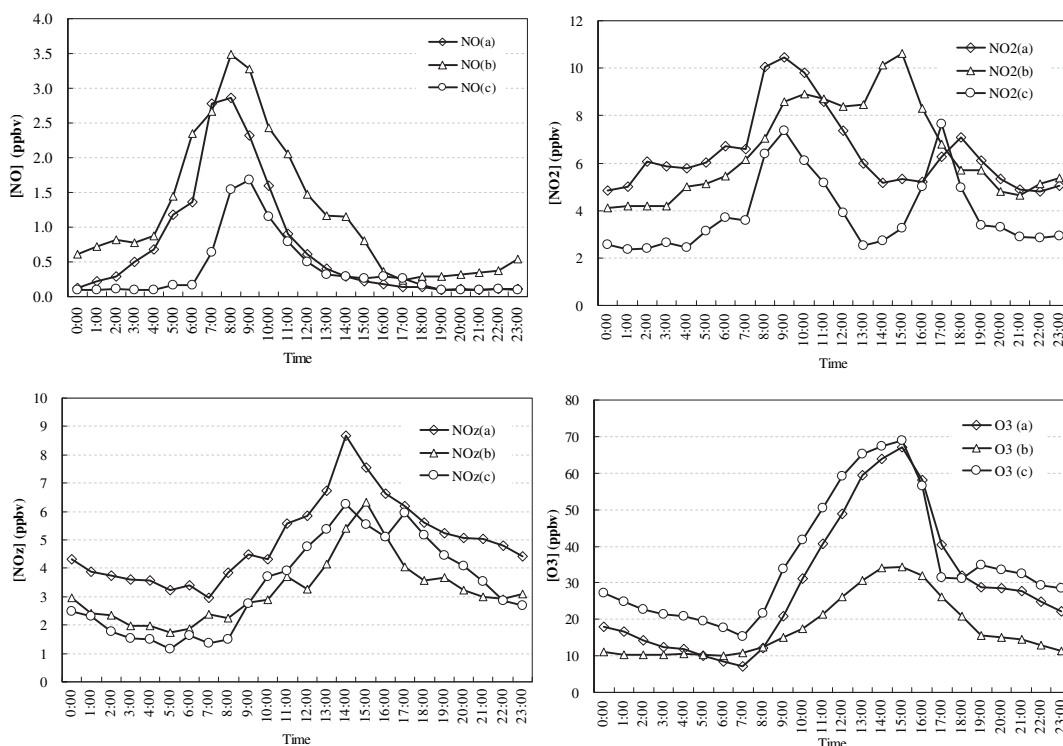


Fig. 3. The daily variations of mean NO, NO₂, NO_x and O₃ in the three stages: (a) first stage; (b) second stage; and (c) third stage.

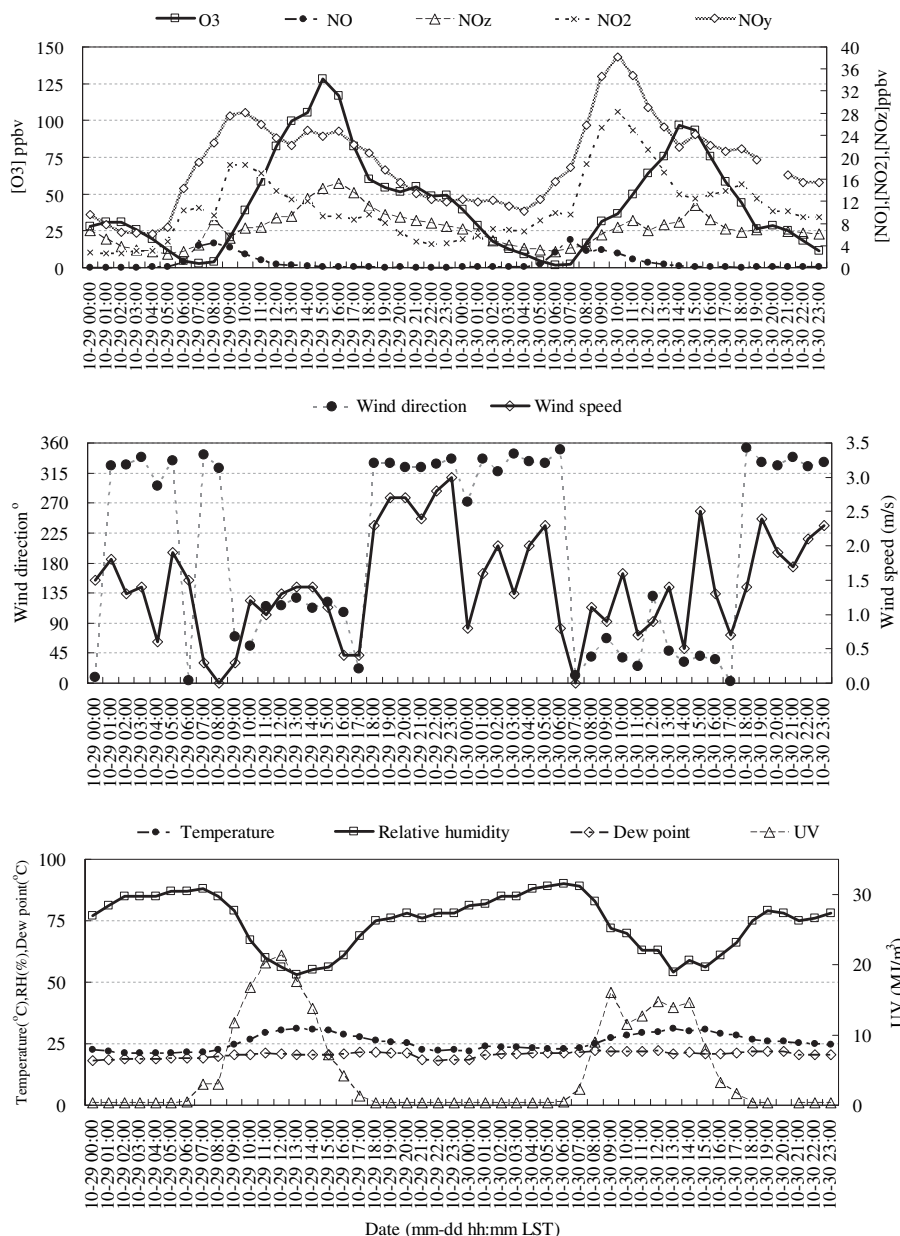


Fig. 4. Time series for the mixing ratios of NO, NO₂, NO_y, NO_z, O₃, and meteorological data during October 29–30th 2008.

the system, and [NO₂] reached their maxima at 1000 LST. Then the photochemical reactions continued to be enhanced, and at 1500 LST the maximum of [O₃] was achieved, with sum of [NO], [NO₂] and [NO_z] reaching a second peak (24.9 ppbv) around 1500 LST, which is due to a superposition effect of complete photochemical reactivity, a continuous rise in oxidation products, the east/south-east direction of the wind, a slight enhancement of wind speed, a drop of [NO₂], and a rise of [NO_z]. The ratio of [NO_z]/[NO_y] continued to increase from morning to noon and then into afternoon, and it was consistent with the increase of [O₃]. Meanwhile the ratio of [NO₂]/[O_x] significantly decreased from the maximum of 80 percent to 6.8 percent. If the NO_z species are the oxidation products of NO_x, the change of composition of NO_y would show the consumption of NO_x due to production of NO_z. [NO] stays below 1 ppbv the levels because far away from the zone of NO emission origin and there are the titration effect of high [O₃]. [NO_z] at 1600 LST reached the maximum level (15.3 ppbv), and the UV radiation

begin to reduce after 1600 LST, accompanied by reduced photochemical production.

In addition, the superposition effects of transport of the smoke plume from the city and the local natural sources need be considered. Urban air pollution transported to more remote areas reaches the ground through the vertical mixing of the mixed layers the next morning after emission. The VOCs are released from rich vegetation in the forests where Observation located, and play an important role in generating O₃ (Chameides et al., 1988; Lamb et al., 1987; Cardelino and Chameides, 1990). It is proven that trees and shrubs can release a large number of isoprenes, α pinene, β pinene, and so on. Different plants release different types of VOCs, and in general, isoprene occupied more than 80 percent of the emissions total. VOCs from plant emissions are more active than anthropogenic emissions, and rapid react with OH could produce a series of photochemical products that could affect NO_x and O₃.

The changes of wind direction were consistent with the fluctuations of air pollutants. Serious pollution of the air was related to the southeasterly winds, and the pollution days of high $[O_3]$ (128 ppbv) had significant effects from the mountain valley breeze such that the photochemical products were transported and aggregated to the mountain areas in daytime, and then the direction of wind was changed, with the polluted air transported back in the evening. Then air pollutants were accumulated in the stable nighttime boundary layer so higher levels of $[NO_2]$ was 7 ppbv and $[NO_y]$ was 129 ppbv were observed in the midnight periods on the 30th. At 0600 LST in the morning of the 30th, the wind direction changed to the east again, which led to rapid buildup of NO_2 and NO_z once more. Both reached maximum values (38.3 ppbv, 28.3 ppbv) at 1000 LST caused by convective transport of air pollutants and the higher accumulation in the previous day. There are precursors with higher concentrations, but the maximal of $[O_3]$ reached 96.5 ppbv, which was lower than the previous day because the solar radiation on that day were 35% lower than that on the 29th, which is due to the sporadic rain in this areas.

3.3. Ozone production efficiency

Ozone production efficiency (OPE) indicates the generated number of O_3 molecules by removal of a molecule of NO_x in an atmospheric photochemical reaction (Liu et al., 1987). NO_x plays a catalytic and circulating role in atmospheric photochemistry of O_3 , but the NO_2 in NO_x would be oxidized to HNO_3 by OH and would be removed from the atmosphere through sedimentation. Therefore, the concept of OPE (NO_x) is a good indicator to assess sensitivity to NO_x or VOCs that generate O_3 and it can gauge the generation of O_3 and be the theoretical basis for a consumption control strategy of O_3 . At the same time, because the OPE (NO_x) not only can be acquired by model calculation but also can be calculated by observational data, it can be a good indicator and also verify model simulation results (Charles et al., 2009).

Analysis of OPE (NO_x) can be directly measured by O_3 , NO_x , and NO_y , and thus the formula establishes a viable method based on the observations for calculating the ozone sensitivity to NO_x . The formulaic expression of OPE (NO_x) has many various forms. Because photolysis of NO_2 during the day quickly produces O_3 , experimental results show that there is a significant linear correlation between O_3 and NO_y and between O_3 and $(NO_y - NO_x)$; here $(NO_y - NO_x)$ stands for the NO_x oxidation products among them (definition: $NO_y - NO_x = HNO_3 + HONO + PAN + \text{other nitrogen oxides} = NO_z$), and OPE (NO_x) is defined as: $OPE(NO_x) = \Delta(O_3 + NO_2) / \Delta(NO_y - NO_x) = \Delta(O_x) / \Delta(NO_z)$ after improved (Nunnermacker et al., 1998; Trainer et al., 1993).

It is generally believed that the further oxidation of NO_x results in NO_z , and NO_z concentration should be increased along with the production process of O_3 . OPE (NO_x) for each day can be calculated with the relationship of growth between $[NO_z]$ and $[O_x]$ ($O_x = O_3 + NO_2$) during the day. In this research, the O_3 production efficiency of NO_x 's was decided by the relationship of $[O_x]$ and $[NO_z]$ within 0800–1400 LST. For example, in the high-ozone pollution case on October 29th and 31st. Fig. 5a, b show scatter diagrams that respectively indicate related changes of $[O_x]$ and $[NO_z]$ on these two days. Obviously, NO_z and O_x have a consistent positive correlation. Fig. 5a, b show the linear correlation between $[O_x]$ and $[NO_z]$ on October 29th, 30th. The slope represents that the average OPE (NO_x) were 10.46 and 15 ppbv/ppbv in these periods. There is a clear change during the day. The values of OPE (NO_x) were comparable with other literature results (Roussel et al., 1996; Li et al., 1997).

The range of reported OPE (NO_x) values is quite large, through the observations and simulated calculation for different regions by scientists from different areas in recent years. Values from the polluted areas average less than 10 (Berkowitz et al., 2004; Carpenter et al., 2000) but in cleaner areas reaches more than 100 (Davis et al., 1996), and also vary because there are many differences due to VOCs, NO_x , atmospheric oxidation, temperature, radiation, and other meteorological factors in different regions' atmospheres. At the same time, a significant variation of OPE (NO_x) in different areas has also been shown in the process of transporting polluted air masses. As an air mass photochemically ages, NO_x is continually oxidized to reduce it from the system, and VOCs control is gradually shifted toward NO_x control, which generates O_3 in the air mass in polluted areas. OPE (NO_x) here maintained a growth trend, so $[O_3]$ rapidly rises in the smoke plume of the city, which results in high $[O_3]$ pollution incidents which often occurred in the large area dozens of kilometers leeward of the city. The observation show that OPEs (NO_x) of high O_3 pollution for these two polluted days were respectively 10.5 and 15, which are more than that for city and lower than that for the clean area. The sensitivity of O_3 generated was transitioning from VOCs control to NO_x control, which is comparable to results from other studies (Roussel et al., 1996; Li et al., 1997).

By the above slope calculation methods, we obtained OPE (NO_x) each day at 0800–1400 LST in the observation period, and extracted the general average of maximum $[O_3]$ in each hour. There is no direct correlation between them, and this is because O_3 can reach its greatest concentration not only by production efficiency, but also by the non-linear relationship with the concentration of its precursors and the ratio, under the same conditions, the initial concentration of the higher NO_x and consumption of reaction cycle

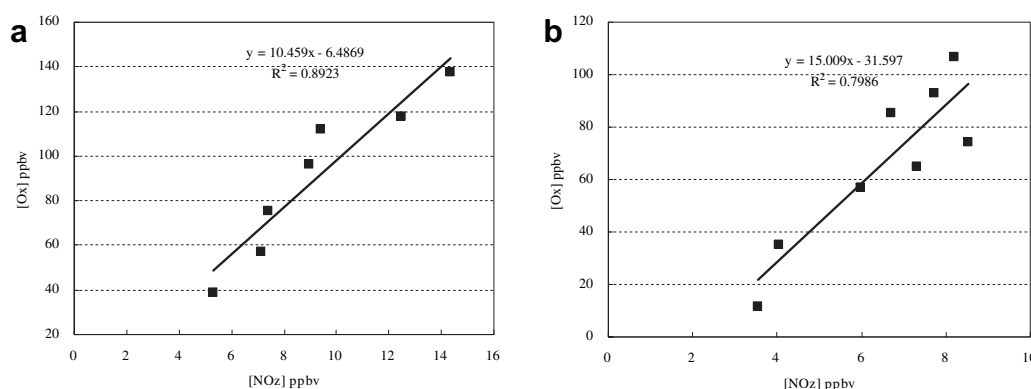


Fig. 5. OPE (NO_x) was determined from the slope of the linear regression of $[O_x]$ versus $[NO_z]$, (a) October 29th 2008 and (b) October 30th 2008.

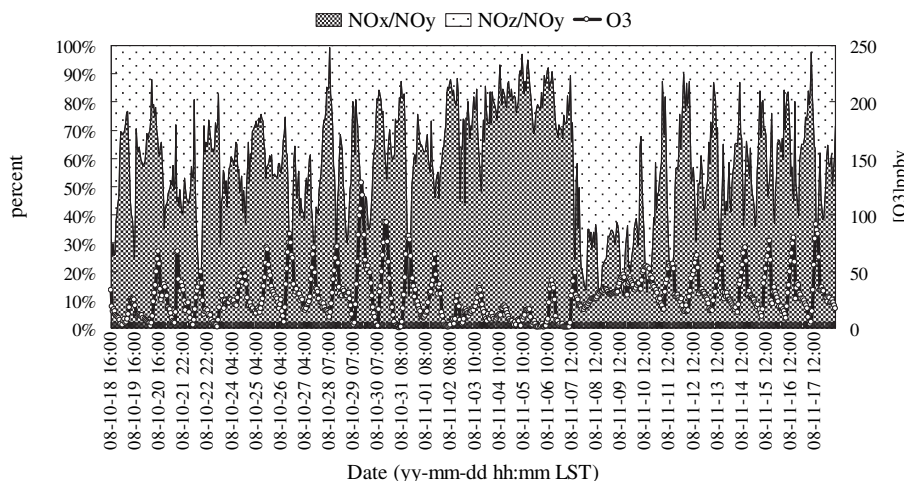


Fig. 6. Time series of [O₃] compared to the partition of NO_y (NO_x and NO_z) during October 18th 2008 to November 17th 2008.

will lead to lower OPE (NO_x). OPE (NO_x) can be a feature from NO_x restriction to NO_x saturation.

Sillman (1995) put forward a guiding value: if [O₃]/[NO_z] < 7, it indicated that VOCs limit O₃ chemistry production. In this study, the OPE (NO_x) was slightly larger than 10 in high O₃ days, which indicated that O₃ production is a transitional state and tend to NO_x control in this region.

3.4. Others photochemical indicators (NO_x/NO_y, NO_z/NO_y, and O₃/NO_x)

In addition to numerical models and the EKMA curve method, photochemical indicator discrimination based on observations has also been widely used. The principle is to evaluate the sensitivity of O₃ generation and observe the chemical properties of air masses by treating the change of concentration ratio between O₃ itself and its precursors as the indicators, such as O₃/NO_y, O_x/NO_y, NO_z/NO_y, H₂O₂/(NO_y–NO_x) and HCHO/NO_y, etc. (Sillman, 1995).

During campaign, as Fig. 6 shows, the low-NO_z/NO_y and high-NO_x/NO_y periods occur almost every morning before 8 o'clock. This means that at this time the atmosphere is in the state of pollutant input, which is due to the mutual effects of the local traffic emissions, convective flow in mixed layers, and NO_z night elimination settling. Between 8:00 and noontime, the NO_z/NO_y ratio increases while the NO_x/NO_y ratio decreases. During this period, [O₃] also increases rapidly. From November 1st to November 6th, the NO_x/NO_y ratio was always high, and there was no significant change in

the day. We checked the meteorological data that there was continuous rain fall during this period, and therefore, the fresh local emissions of pollutants could not easily out and photochemical reactions were weak. From November 8th to November 10th, the NO_z/NO_y ratio was always high, and according to meteorological data, there was a transit of continuous northly wind, which brought about the comparatively aged air mass and the active precursors of the lower concentration air mass, plus the favorable local diffusion conditions which led to the insignificant diurnal variation in [O₃] over several days (see Fig. 7).

Therefore, the relevant indicators developed from the concentration of NO_y and NO_z and the ratios NO_x/NO_y and NO_z/NO_y can be used to analyze the simulation results to explore the role and impact of O₃ photochemical pollution in the transport process.

The interactions Δ(O₃)/Δ(NO_x) as a characterization of O₃ generation and the elimination of NO_x from the system show NO₂ in the NO_x pool will cycle in the photochemical reactions, and at the same time react with VOCs free radicals to generate NO_z and be eliminated from the system. In the two high-ozone events 0900 LST to 1300 LST in October 19th and 30th a scatter diagram correlation analysis of the [O₃] and [NO_x] data show a linear relationship, Fig. 8 shows that these two days' [O₃] and [NO_x] data showed a strong negative correlation. R² values reached 0.9879 and 0.994 respectively, and the slopes were respectively –0.125 and –0.31. On October 29th, although the maximum hourly mean [O₃] was higher than that on the 30th, the generation of O₃ and the reduction of NO_x on the 30th was faster. It can be seen from the conclusions of

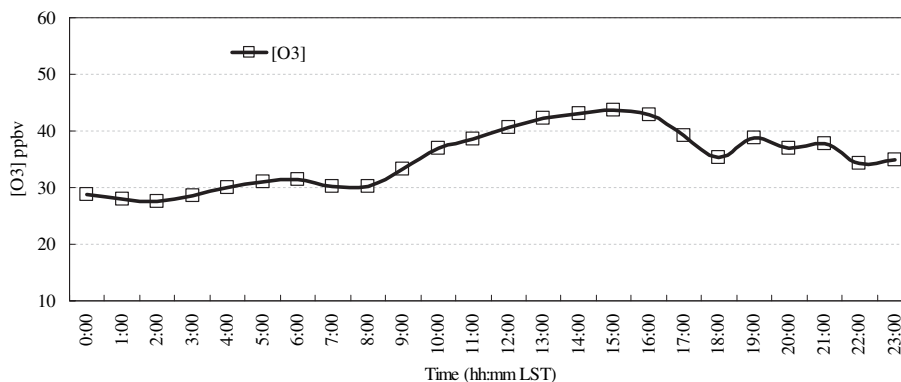


Fig. 7. The average diurnal variation of O₃ from November 7th to November 10th.

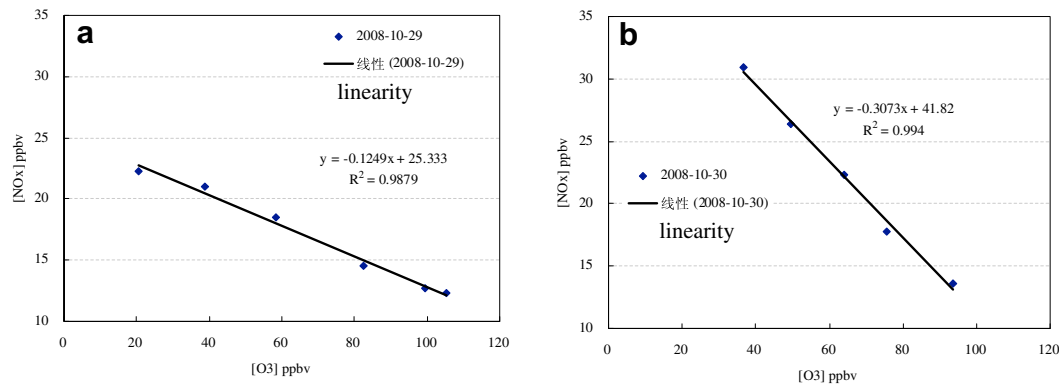


Fig. 8. Correlation analysis of $[O_3]$ and $[NO_x]$: (a) October 29th 2008 and (b) October 30th 2008.

Section 3.3, the OPE (NO_x) value for the 30th was higher, which means that the NO_x generation of O_3 was more efficient. But the 30th NO_x was eliminated more and faster from the system. However, the results are actually not contradictory. By analyzing the OPE (NO_x), we can see that on the 29th, the elimination path way of NO_x was through the reacting and generating NO_z and then proceeding to elimination by settlement, but on the 30th the elimination process of NO_x did not generate more NO_z , which means that NO_x was eliminated before it participated in the photochemical reactions. The meteorological data indicate that there was less radiation on the 30th and the turbulent diffusion was weaker than that on the 29th. Further, the surrounding weather pattern featured light rain, so that the direct elimination ratio of NO_x was higher. Therefore, the non-linear relationship between NO_x and O_3 also stems from the non-linear features of various meteorological factors.

3.5. Smog production model

The Smog Production Model (SPM) is a semi-empirical formulation, which is based on O_3 and NO_x to observe the degree of photochemical reaction and decide which restricts O_3 more, between VOCs or NO_x . It was firstly studied by the Graham Johnson team in Australia (1984), and then by Blanchard et al. (1993); Chang and Rudy (1993) who observed smog chamber data to amend parameters of the basic assumptions in the SP algorithm to improve the accuracy for forecasting ozone sensitivity (VOCs or NO_x control). In this study, the application of SPM is to assess sensitivity of O_3

qualitatively in the region and the effect of the relative trends between VOCs and NO_x control.

Explanations for the SPM results are that when reaction levels are less than 0.6 it represents the system is strongly VOCs limited, when reaction level is between 0.6 and 0.9, transition to NO_x control, and at reaction levels more than 0.9, it stands for strong NO_x control. In prior studies, NO_x environmental monitoring by standard equipment (to measure NO_2 by the molybdenum conversion method) generated great errors by the inclusion of HNO_3 , PAN, and some NO_x in the measured value. These measured values not only capture molecules which are not NO_x , but also aren't realistically NO_y either. However, in this study, NO_2 was measured by light conversion to obtain precise NO_x concentrations, and thus more accurate decisions about control over ozone production will be obtained with this method.

Through the calculation of average data of O_3 , NO , and NO_2 per hour during daytime, time series of these parameters related to reaction level and the value of $[O_3]$ were obtained together. From Fig. 9, we can see that the parameters of reaction level indicate values of less than 0.6 over 17 day, and reaction levels of more than 0.6 occupied 13 days. However, there are zero days with extent values more than 0.8, which shows the observation station is not a NO_x -sensitive system during the observation period. The high- O_3 event is a transition state from VOCs sensitivity to NO_x sensitivity on Oct. 29th, which is consistent with the analysis result of OPE (NO_x) in Section 3.3, which shows that the generation of high- O_3 was influenced by a city smog plume. Through analysis of the extent of reaction and wind data

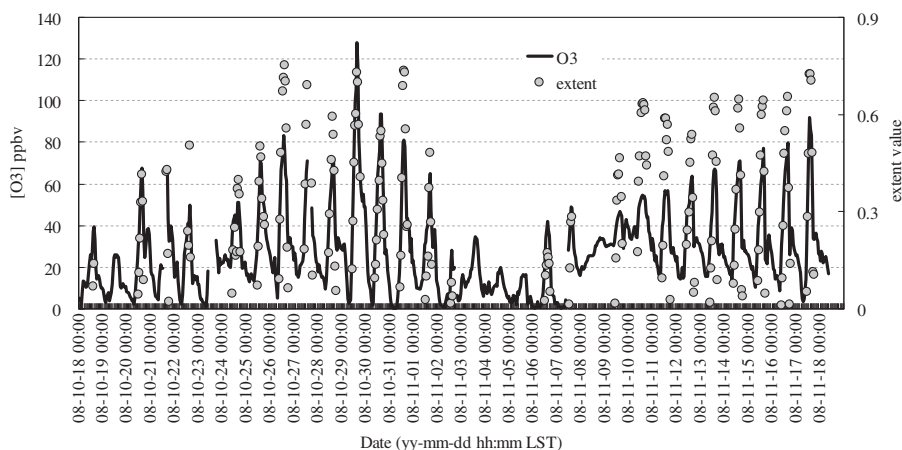


Fig. 9. Time series of $[O_3]$ and extent during the 2008 campaign period.

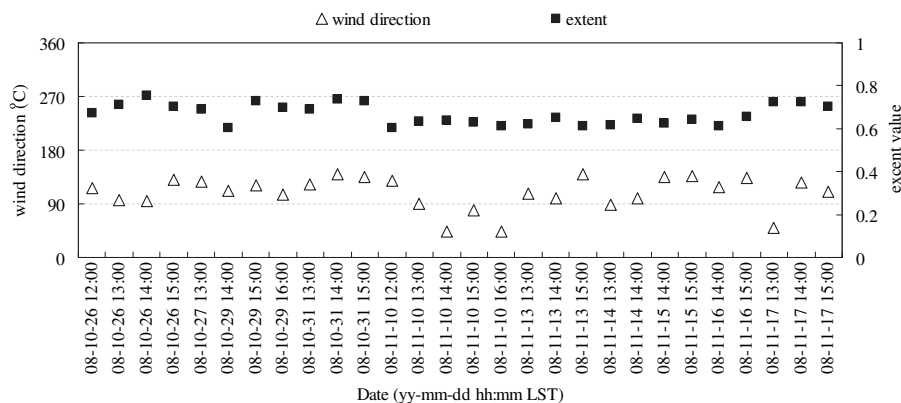


Fig. 10. Analysis of extent of reaction and wind data (when extent of reaction >0.6).

(Fig. 10), when extent of reaction is greater than 0.6, the wind direction is generally southeasterly. It implies the southeast winds bring the photochemical aged air mass in the fall.

4. Conclusions

There are photochemical pollution episodes with high $[O_3]$ (128 ppbv hourly) in Dinghushan area observed in autumn, when the area is controlled by a strong subtropical high and when temperature is high and relative humidity is low. The data show a pollution episode caused by superposition of local photochemical reactions and the regional transport.

The data show that OPE (NO_x) of high O_3 pollution during observation period was slightly larger than 10, which is more than in city and lower than remote clean. This indicates that the sensitivity of O_3 generated was based on a transition from a VOCs control to a NO_x control.

When there was a transit of continuous north wind, which brought about the comparatively aged air mass, the active precursors of the lower concentration air mass and the good local diffusion conditions led to an insignificant diurnal variation and low value ozone.

The SPM results also imply that the high- O_3 event is a transition state from VOCs sensitivity to NO_x sensitivity, and the generation of high- O_3 was influenced by a city smog plume. It shows the photochemical pollution at the observation station is mostly subject to southeasterly air flow influence in the fall.

Acknowledgments

I would like to thank Senior Engineer Liu Guangren for providing a great deal of assistance in the completion of the experiments. The work presented in this paper was supported by the National Key Basic Research and Development Plan (973 project) (2007CB407303), the grant of the Knowledge Innovation Program of Chinese Academy of Sciences (approved # KZCX1-YW-06-01) (IAP07416), China Postdoctoral Science Foundation (20060400743) and the Hi-tech Research and Development Program of China (Grant No. 2006AA06A301).

References

Ariel, F.S., Mantilla, E., Millán, M., 2005. Using measured and modeled indicators to assess ozone- NO_x -VOCs sensitivity in a western Mediterranean coastal environment. *Atmos. Environ.* 39, 7167–7180.

Berkowitz, C.M., Jobson, T., Jiang, G., et al., 2004. Chemical and meteorological characteristics associated with rapid increases of O_3 in Houston. *Texas. J. Geophys. Res.* 109 (D10), 307. doi:10.1029/2003JD004141.

Blanchard, C.L., Roth, P.M., Jeffries, H.E., 1993. Spatial mapping of preferred strategies for reducing ambient ozone concentrations nationwide. In: Paper Presented at the 86th Annual Meeting of Air & Waste Management Association.

Cardelino, C.A., Chameides, W.L., 1990. Natural hydrocarbon, urbanization, and urban ozone. *J. Geophys. Res.* 95 (D9), 13971–13979.

Carl, M., Berkowitz, R.A., Bian, Z.X., Zhong, S., Robert, S., Disselkamp, N.S., Laulainen, E.G.C., 2001. Aircraft observations of aerosols, O_3 and NO_y in a nighttime urban plume. *Atmos. Environ.* 35, 2395–2404.

Carpenter, K., Stehr, J.W., et al., 2000. Observations of NO_y , CO , and SO_2 and the origin of reactive nitrogen in the eastern United States. *J. Geophys. Res.* 105, 3553.

Cassandra, V.H., Munger, J.W., Steven, C.W., Zahniser, M., Nelson, D.J., McManus, B., 2006. Atmospheric reactive nitrogen concentration and flux budgets at a Northeastern U.S. forest site. *Agr. Forest Meteorol.* 136, 159–174.

Chameides, W.L., Lindsay, R.W., Richardson, J., Kiang, C.S., 1988. The role of Biogenic Hydrocarbons in urban photochemical Smog Atlanta as case study. *Science* 241, 1473.

Chang, T.Y., Rudy, S.J., 1993. Ozone-precursor relationships: a modeling study of semi-empirical relationships. *Environ. Sci. Technol.* 27, 2213–2219.

Charles, C.K., Chou, C.Y.T., Chein, J.S., Liu, S.C., Zhu, T., 2009. Measurement of NO_y during campaign of air Quality research in Beijing 2006 (CAREBeijing-2006): implications for the ozone production efficiency of NO_x . *J. Geophys. Res.* 114, D00G01. doi:10.1029/2008JD010446.

Davis, D.D., Crawford, J., Chen, G., et al., 1996. Assessment of ozone photochemistry in western North Pacific as inferred from PEM-West A observations during fall 1991. *J. Geophys. Res.* 101, 2111–2134.

Guangfeng, J., Jerome, D.F., 2004. Modeling the effects of VOCs and NO_x emission sources on ozone formation in Houston during the TexAQs 2000 field campaign. *Atmos. Environ.* 38, 5071–5085.

Lamb, B., Guenther, A., Gay, D., Westberg, H., 1987. A National Inventory of Biogenic hydrocarbon emissions. *Atmos. Environ.* 21 (8), 1695–1705.

Li, S.M., Anlauf, K.G., Wiebe, H.A., et al., 1997. Emission ratios and photochemical production efficiencies of nitrogen oxides, ketones, and aldehydes in the lower Fraser Valley during the Summer Pacific 1993 Oxidant study. *Atmos. Environ.* 31, 2037–2048.

Liu, S.C., Trainer, M., Fehsenfeld, F.C., et al., 1987. Ozone production in the rural troposphere and the implications for regional and global ozone distributions. *J. Geophys. Res.* 92, 4191–4207.

Mannschreck1, K., Gilge, S., Duellmer, P.C., Fricke, W., Berresheim, H., 2004. Assessment of the applicability of NO_2 - O_3 photostationary state to long-term measurements at the Hohenpeissenberg GAWStation, Germany. *Atmos. Chem. Phys.* 4, 1265–1277.

Moore, T.C., Lee, J., Sullivan, P.A., Roelle, V., Aneja, P., 2001. Vertical distribution of oxides of nitrogen in the semi-urban planetary boundary layer: mixing ratios, sources and transport. *Chemosphere Global Change Sci.* 3, 7–23.

Nunnermacker, L.J., Imre, D., Daum, P.H., et al., 1998. Characterization of the Nashville urban plume on July 3 and July 18, 1995. *J. Geophys. Res.* 103, 28129–28148.

Paul, O., Wennberg, Donald, D., 21 March 2008. Rethinking ozone production. *Science* 319.

Penga, Y.P., Chena, K.S., Laib, C.H., Lua, P.J., Kaoa, J.H., 2006. Concentrations of H_2O_2 and HNO_3 and O_3 -VOCs- NO_x sensitivity in ambient air in southern Taiwan. *Atmos. Environ.* 40, 6741–6751.

Raivonen, M., Vesala, T., Pirjola, L., Altimir, N., Keronen, P., Kulmala, M., Hari, P., 2009. Compensation point of NO_x exchange: net result of NO_x consumption and production. *Agr. Forest Meteorol.* 49, 1073–1081.

Russel, P.B., Lin, X., Camacho, F., et al., 1996. Observations of ozone and precursors at two sites around Toronto, Ontario, during SONTOS 92. *Atmos. Environ.* 30, 2145–2155.

Sillman, S. The use of NO_y , H_2O_2 and HNO_3 as indicators for ozone- NO_x -hydrocarbon sensitivity in urban locations. 1995 *J. Geophys. Res.* 100, 14175–14188.

- Thomas, A.V., Berg, M., Heil, T., Houben, A.N., Lerner, W., Petrick, D.R., Pätz, H.W., 2005. Measurements of total odd nitrogen (NO_y) aboard MOZAIC in-service aircraft: instrument design, operation and performance. *Atmos. Chem. Phys.* 5, 583–595.
- Trainer, M., Parrish, D.D., Buhr, M.P., et al., 1993. Correlation of ozone with NO_y in photochemically aged air. *J. Geophys. Res.* 98, 2917–2985.
- Wang, T., Lam, K.S., Lee, A.S.Y., 1998. Meteorological and chemical characteristics of the photochemical ozone episodes observed at Cape D'Aguilar in Hong Kong[J]. *J. Appl. Meteorol.* 37 (10), 1167–1178.
- Zhang, L., Wiebe, A., Vet, R., Mihele, C., Jason, M., Brien, O., Iqbal, S., Liang, Z., 2008. Measurements of reactive oxidized nitrogen at eight Canadian rural sites. *Atmos. Environ.* 42, 8065–8078.